The forced oscillator method: Its applications to physical systems

Tsuneyoshi Nakayama and Hiroyuki Shima
Department of Applied Physics, Hokkaido University

The forced oscillator method (FOM) is particularly suitable to treat very large matrices by using advanced modern supercomputers. This method enables us to calculate in an efficient way spectral densities, eigenvalues, and their eigenvectors of large-scale matrices. In addition, linear response functions of systems described by these matrices can be computed by the FOM. We have also developed the finite-time scaling approach to obtain the precise value of dynamical exponents with less computational effort. It is shown that the power law behavior $\sigma(\omega) \propto \omega^{1/3}$ is hold in the critical region of the metal-insulator transition for 3D Anderson systems.

1. Introduction

The importance of eigenvalue analysis of very large matrices has been well recognized in many fields of science and engineering. As sizes of matrices become large, calculations by conventional methods are difficult, since the computing time as well as the memory space grows very rapidly. So far, many algorithms, suitable to treat very large matrices, have been developed. Among these, the forced oscillator method (FOM) offers a powerful way handling very large $N \times N$ matrices, namely computing accurately spectral densities, eigenvalues, and their eigenvectors of very large matrices. The FOM was initially proposed for obtaining eigenvalues and their eigenvectors of a lattice dynamical problem described by Hermitian matrices.[1,2] The FOM has been extended in order to treat large-scale non-Hermitian matrices.[3] It is now possible to treat not only the eigenvalue problems of lattice dynamics, but also of the general type of matrices by mapping them onto those of lattice dynamics.[4]

Particular advantages of the FOM lie on being easily vectorized for implementation on an array- or parallel-processing modern supercomputer. This is due to the fact that a time-consuming part in the computation is to solve the equation of motion and the program is easily optimized. It is becoming common by this method to treat matrices with $N \sim 10^7$ or more. The FOM enables us to calculate the linear response functions of quantum systems.[5] The method is broadly applicable and may be of importance in a variety of physical systems.

Using this technique, we have investigated the dynamic scaling behavior of ac conductivity $\sigma(\omega)$ in three dimensional (3D) Anderson systems. A new scaling approach has been proposed, utilizing the characteristics of the FOM, to determine the dynamical exponent of the ac conductivity $\sigma(\omega) \propto \omega^{\delta}$ near the Anderson transition with high speed and accuracy.[6,7] This paper we presents the algorithm to calculate the Kubo-Greenwood formula[8] of ac conductivity $\sigma(\omega)$, and demonstrate the numerical results of $\sigma(\omega)$ near the Anderson transition which behave as $\sigma(\omega) \propto \omega^{\delta}$ ($\delta \simeq 1/3$) for all of universality classes.

The outline of this paper is as follows. Section 2 gives the efficient algorithm for computing linear response functions of quantum systems. In Section 3, we apply this algorithm to calculate the Kubo-Greenwood formula of ac conductivity. Section 4 shows the calculated results of $\sigma(\omega)$ for the 3D Anderson model near the transition. Section 5 presents the finite-time scaling method for the dynamical exponent of $\sigma(\omega) \propto \omega^{\delta}$. A summary is given in Section 6.

2. Linear response functions for quantum systems

Linear response function are quite important to gain insight into dynamical properties of quantum systems. Calculations of linear response functions for quantum systems described by $N \times N$ Hamiltonian matrices normally require the evaluation of all eigenvalues and corresponding eigenvectors. As sizes of matrices become large, standard diagonalization routines require a large amount of the computing time proportional to $O(N^3)$ as well as memory space proportional to $O(N^2)$. They remain limited to systems of modest size because of the high computational cost.

We have developed the algorithm based on the FOM to calculate linear response functions of quantum systems described by large-scale Hamiltonian matrices. The advantages of this method compared to existing methods are that (1) it requires memory space of the order of N for sparse matrices, (2) the computing time is proportional to N^2, and (3) it is easily vectorized and parallelized for implementation in an array-processing modern supercomputer. The last advantage is due to the fact that the time-consuming part in computations is to solve equations of motion and the program is easily optimized.

Consider a quantum system described by

$$\hat{H} = \sum_{mn} K_{mn} |m\rangle\langle n| \quad (m, n = 1, 2, \ldots, N), \tag{1}$$

where $\langle m|$ is the bra vector in an *arbitrary* notation. Since the set $\{|m\rangle\}$ satisfies the closure relation $\sum_m |m\rangle\langle m| = 1$, an arbitrary state is expressed as

$$|\Psi(t)\rangle = \sum_m a_m(t)|m\rangle. \tag{2}$$

We impose a small perturbation $\hat{V}$ to the system expressed

by

$$\hat{V} = -\frac{1}{2}\sum_{\alpha} \hat{x}_{\alpha}(f_0^{\alpha}\mathrm{e}^{-\mathrm{i}\omega t} + \mathrm{c.c.}), \tag{3}$$

where $\hat{x}_\alpha$ is the α component of the *generalized* displacement and f_0^α is the corresponding generalized force. c.c. indicates a complex conjugate. Substituting Eqs. (1) and (3) into the Schrödinger equation for $|\Psi(t)\rangle$ and multiplying by $\langle k|$ from the felt, one has the inhomogeneous coupled linear differential equation

$$\mathrm{i}\hbar\frac{da_m(t)}{dt} - \sum_n K_{mn}a_n(t) = \sum_{\alpha}\sum_n V_{mn}^{\alpha}(t)a_n(t). \tag{4}$$

For a small perturbation, the time-dependent first-order perturbation theory is applicable by putting $a_m(t) = a_m^{(0)}(t) + \sum_\alpha a_{m\alpha}^{(1)}(t)$ into Eq. (4). The first-order equation becomes

$$\begin{aligned}\mathrm{i}\hbar\frac{da_{m\alpha}^{(1)}(t)}{dt} &- \sum_n K_{mn}a_{n\alpha}^{(1)}(t) \\ &= -\frac{\hbar}{2}(F_{m\alpha}\mathrm{e}^{-\mathrm{i}\omega t} + \tilde{F}_{m\alpha}\mathrm{e}^{\mathrm{i}\omega t})\mathrm{e}^{-\mathrm{i}\omega_{\lambda_0}t}.\end{aligned} \tag{5}$$

Here

$$F_{m\alpha} = \sum_n \frac{f_0^{\alpha}}{\hbar}x_{mn}^{\alpha}u_n(\lambda_0), \tag{6}$$

$$\tilde{F}_{m\alpha} = \sum_n \frac{f_0^{\alpha *}}{\hbar}x_{mn}^{\alpha}u_n(\lambda_0), \tag{7}$$

where $u_m(\lambda_0) \equiv \langle m|\omega_{\lambda_0}\rangle$ is the mth element of the initial eigenvector belonging to the eigenvalue ω_{λ_0} of the matrix $\{K_{mn}\}$. Here we assume that the unperturbed state is given by $a_m^{(0)}(t) = u_m(\lambda_0)\mathrm{e}^{-\mathrm{i}\omega_{\lambda_0}t}$.

Let us introduce the "resonance" function defined by

$$E_{\alpha\beta}(\Omega, t) = \sum_m a_{m\alpha}^{(1)*}(t)a_{m\beta}^{(1)}(t). \tag{8}$$

By substituting the solution of Eq. (5) into Eq. (8), one has

$$E_{\alpha\beta}(\Omega, t) = \sum_{\lambda}\left|\sum_m F_{m\alpha}u_m^*(\lambda)\right|^2 \frac{\sin^2\{(\omega_\lambda - \Omega)t/2\}}{(\omega_\lambda - \Omega)^2}, \tag{9}$$

where $\Omega = \omega_{\lambda_0} + \omega$, and the contribution from the second term on the right hand side of Eq. (5) is ignored since we consider the case of zero temperature (see Ref. 5). The eigenvectors contributing to the sum in Eq. (9) are those whose frequencies lie within about $\pm(2\pi/T)$ of Ω, where T is the time interval. Suppose that the following conditions are satisfied:

$$\frac{1}{\Omega} \ll T \ll \frac{4\pi}{\Delta\omega}, \tag{10}$$

where $\Delta\omega$ is the average eigenfrequency spacing. Taking a proper time interval T satisfying the condition Eq. (10), Eq. (9) gives

$$\begin{aligned}E_{\alpha\beta}(\Omega, T) = &\frac{\pi T f_0^{\alpha *}f_0^{\beta}}{2\hbar^2}\sum_{\lambda}\langle\omega_{\lambda_0}|\hat{x}_{\alpha}|\omega_\lambda\rangle \\ &\times\langle\omega_\lambda|\hat{x}_{\beta}|\omega_{\lambda_0}\rangle\delta(\omega_\lambda - \Omega),\end{aligned} \tag{11}$$

where the following representation was used;

$$\sum_m F_{m\alpha}u_m^*(\lambda) = \frac{f_0^{\alpha}}{\hbar}\langle\omega_\lambda|\hat{x}_{\alpha}|\omega_{\lambda_0}\rangle. \tag{12}$$

The generalized susceptibility $\chi_{\alpha\beta}(\omega)$ is given by the Kubo formula [9] under the generalized external force defined in Eq. (3),

$$\chi_{\alpha\beta}(\omega) = \frac{\mathrm{i}}{\hbar}\int_0^{\infty}\mathrm{e}^{\mathrm{i}\omega t}\langle[\hat{x}_{\alpha}(t), \hat{x}_{\beta}(0)]\rangle dt, \tag{13}$$

where angular brackets denote the thermal average. At the zero temperature, the imaginary part of the generalized susceptibility for a given initial state $|\omega_{\lambda_0}\rangle$ is expressed by

$$\chi''_{\alpha\alpha}(\omega) = \frac{\pi}{\hbar}\sum_{\lambda}|\langle\omega_{\lambda_0}|\hat{x}_{\alpha}|\omega_\lambda\rangle|^2\,\delta(\omega_{\lambda\lambda_0} - \omega) \tag{14}$$

where $\omega_{\lambda\lambda_0} = \omega_\lambda - \omega_{\lambda_0}$. Choosing $f_0^\alpha = 1$, $\chi''_{\alpha\alpha}(\omega)$ can be expressed by the resonance function given by Eq. (11) as

$$\chi''_{\alpha\alpha}(\omega) = \frac{2\hbar E_{\alpha\alpha}(\Omega, T)}{T}. \tag{15}$$

This relation is the key equation that relates the resonance function $E_{\alpha\alpha}(\Omega, T)$ to the imaginary part of the generalized susceptibility $\chi''_{\alpha\alpha}(\omega)$.

3. Computing the Kubo-Greenwood formula

This Section describes the relationship between the Kubo-Greenwood formula for the ac conductivity and the resonance function defined by Eq. (8) via the imaginary part of the generalized susceptibility $\chi''(\omega)$.

The generalized conductivity is expressed as [9]

$$\Sigma(\omega) = \frac{1}{\hbar\omega L^d}\lim_{\varepsilon\to 0}\int_0^{\infty}\mathrm{e}^{\mathrm{i}\omega t - \varepsilon t}\langle[\hat{J}(t), \hat{J}(0)]\rangle dt, \tag{16}$$

where $\hat{J}(t)$ is the current operator and the angular brackets mean the thermal average. From this one can derive the ac conductivity $\sigma(\omega)$ by setting $\hat{x} = \hat{J}$ in Eq. (14). Taking account of the Fermi distribution function $f(\omega)$ at $T = 0$, the ac conductivity $\sigma(\omega)$ is expressed by the imaginary part of the generalized susceptibility $\chi''(\omega)$ as

$$\begin{aligned}\sigma(\omega) &= \frac{2}{\omega L^d}\sum_{\omega_{\lambda_0}}\chi''(\omega)[f(\omega_{\lambda_0}) - f(\omega_{\lambda_0} + \omega)] \\ &= \frac{2}{\omega L^d}\sum_{\omega_{\lambda_0}=\omega_{\mathrm{F}}-\omega}^{\omega_{\mathrm{F}}}\chi''(\omega),\end{aligned} \tag{17}$$

where the spin freedom is taken into account and the definition of the Fermi frequency is $\omega_{\mathrm{F}} = E_{\mathrm{F}}/\hbar$. The meaning of $\sum_{\omega_{\lambda_0}=\omega_{\mathrm{F}}-\omega}^{\omega_{\mathrm{F}}}$ is the sum over the initial state $|\omega_{\lambda_0}\rangle$ at zero temperature. Equation (17) is shown to be equivalent to the Kubo-Greenwood formula as follows: Equation (17) can be rewritten as

$$\sigma(\omega) = \frac{2}{\omega}\int_{E_{\mathrm{F}}-\hbar\omega}^{E_{\mathrm{F}}} dE_{\lambda_0}\mathcal{D}(E_{\lambda_0})\chi''(\omega), \tag{18}$$

where $\mathcal{D}(E_{\lambda_0})$ means the spectral density of states (DOS) at the eigenenergy $E_{\lambda_0} = \hbar\omega_{\lambda_0}$. Substituting Eq. (14) into

Eq. (18), one has,

$$\sigma(\omega) = \frac{2\pi e^2}{\hbar\omega}\sum_{\omega_\lambda}\Big\{\int_{E_{\rm F}-\hbar\omega}^{E_{\rm F}} dE_{\lambda_0}\,|\langle\omega_\lambda|\hat{v}|\omega_{\lambda_0}\rangle|^2 \times \mathcal{D}(E_{\lambda_0})\delta(\omega_{\lambda_0}+\omega-\omega_\lambda)\Big\}, \tag{19}$$

where $\hat{v}$ is the velocity operator. The use of the relation $\Sigma_\lambda = L^d\int\mathcal{D}(E_\lambda)dE_\lambda$ in Eq. (19) yields

$$\sigma(\omega) = 2\pi e^2\hbar L^d\int_{E_{\rm F}-\hbar\omega}^{E_{\rm F}} dE_{\lambda_0}\frac{|\langle\omega_{\lambda_0}+\omega|\hat{v}|\omega_{\lambda_0}\rangle|^2}{\hbar\omega} \times \mathcal{D}(E_{\lambda_0})\mathcal{D}(E_{\lambda_0}+\hbar\omega). \tag{20}$$

This is the Kubo-Greenwood formula.[8)]

From Eqs. (15) and (17), the explicit form of the ac conductivity, expressed by the resonance function given by Eq. (8), becomes

$$\sigma(\omega) = \frac{4\hbar}{\omega T L^d}\sum_{\omega_{\lambda_0}=\omega_{\rm F}-\omega}^{\omega_{\rm F}} E(\Omega,T), \tag{21}$$

where the time T satisfies the condition $1/\Omega \ll T \ll 4\pi/\Delta\omega$. We should emphasize that the accuracy of the calculated results becomes better as the system size N increases since many modes are included in the resonance width $4\pi/T$.

4. AC conductivity of disordered electron systems

In order to assess the efficiency of this algorithm, we consider noninteracting electron systems with disordered potentials. The metal-insulator transition in disordered electron system is called the Anderson transition,[10)] and their critical behavior are classified into three universality classes according to the basic symmetry of the Hamiltonian, namely, the orthogonal, the unitary, and the symplectic classes.[11)] The $\omega^{1/3}$ dependence of $\sigma(\omega)$ at the 3D Anderson transition was predicted by Wegner[12)] using the single-parameter scaling hypothesis, but this dependence was not verified numerically until the work by Lambrianides and Shore.[13)] They evaluates the Kubo-Greenwood formula for orthogonal systems by directly calculating eigenvectors of the order of 10^5 for system sizes $L = 6-14$ and by pulling out the DOS $\mathcal{D}(\omega_{\lambda_0})$ and $\mathcal{D}(\omega_{\lambda_0}+\omega)$ from the integral in Eq. (19). We do not need to do so to calculate the ac conductivity since the information on the DOS is automatically involved in our algorithm though Eq. (9).

We have investigated the dynamical exponents in 3D unitary and symplectic systems in addition to orthogonal one. For these systems different from orthogonal one, the Hamiltonian matrices become complex and/or posses spinor components so that it is not easy to calculate $\sigma(\omega)$ with conventional methods. Within our knowledge, the present work is the first numerical realization of the $\omega^{1/3}$-behavior of $\sigma(\omega)$ in unitary and symplectic systems.[7)]

The Hamiltonian of the system is given by

$$H = \sum_{i,\sigma} W_{i,\sigma}\,|i\sigma\rangle\langle i\sigma| + \sum_{i,\sigma;j,\sigma'} V_{i,\sigma;j,\sigma'}\,\big|i\sigma\rangle\langle j\sigma'\big|, \tag{22}$$

where i denotes the lattice site, and σ the spin, respectively. We set the lattice constant to be unity and only the nearest neighbor coupling is taken into account. The on-site potentials $\{W_i\}$ are assumed to be distributed independently, and the distribution is taken to be uniform in the range $[-W/2, W/2]$. In the orthogonal case, $V_{i,\sigma;j,\sigma'} = V\delta_{\sigma,\sigma'}$ is real, while $V_{i,\sigma;j,\sigma'}$ is $V\exp(i\phi_{i,j})\,\delta_{\sigma,\sigma'}$ in the unitary case with the Peierls phase factor $\phi_{i,j}$. In both cases, no spin flip process is included. In the symplectic case, the hopping energy is described by

$$V_{i,\sigma;i-k,\sigma'} = V\left[\exp\left(-i\theta\sigma_k\right)\right]_{\sigma,\sigma'}, \quad k \equiv \hat{x},\hat{y},\hat{z} \tag{23}$$

where σ_k are Pauli matrices.[14)] We set the hopping amplitude V the energy unit.

In order to discuss the dynamic properties in the vicinity of the Anderson transition, we set the disorder strength $W = W_C = 16.5$ for an orthogonal case,[15)] and $W_C = 17.9$ for an unitary case,[16)] assuming uniform magnetic flux penetrating through a x-y plane unit cell is set to be 0.2 times the flux quantum. For symplectic case, we set $\theta = \pi/6$ in Eq. (23), and W is set to the critical value $W_C = 19.0$.[17)] The Fermi energy E_F is fixed to the band center. Actual simulations have been performed for systems with $30\times30\times30$ lattice sites for all cases. In each case, averaging over 20 independent realization of random potentials has been performed.

Figure 1 presents the calculated results of $\sigma(\omega)$ for symplectic cases taking various time interval $T = \pi/2$–200π. The corresponding resonance widths become $4\pi/T = 0.02$–8.0 in units of $V = 1$. We see from Fig. 1 that the calculated results follow the $\omega^{1/3}$-behavior with increasing time interval T over two orders of magnitude on frequency. The results for orthogonal and unitary case are quite similar to Fig. 1 (see Ref. 7 and references therein).

5. Finite-time scaling approach

In this section we present the finite-time scaling approach for determine the critical exponent of the ac conductivity $\sigma(\omega) \propto \omega^\delta$ and the calculated results of δ for unitary and

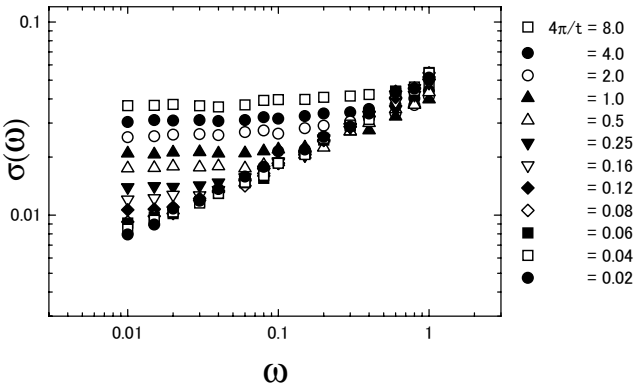

Fig. 1. Calculated ac conductivity $\sigma(\omega)$ near the 3D Anderson transition for symplectic system. Time duration dependence is shown.

symplectic systems. This scaling approach is based on the fact that the number of eigennmodes contributing to the sum on λ in Eq. (9) depends on the resonance width of sinclike function $4\pi/T$, which is inversely proportional to the time interval T for which the external force is applied.

As mentioned in Section 4, the 3D Anderson model described by Eq. (22) exhibits the metal-insulator transition, and the ac conductivity $\sigma(\omega)$ at the transition point ($W = W_{\rm c}$ and $\hbar\omega_{\rm F} = 0$) follows

$$\sigma(\omega) \propto \omega^{\delta}, \tag{24}$$

with $\delta = 1/3$. Since the DOS near $\omega_{\rm F} = 0$ (the critical point) is almost constant, there is no characteristic energy at criticality. Therefore, only the time interval T characterizes the time scale of the system. Thus, the T-dependent ac conductivity can be assumed to be written in the scaling form:

$$\sigma(\omega, T) = T^{-\delta} G(\omega T), \tag{25}$$

where the asymptotic form of $G(z)$ should be

$$G(z) \propto \begin{cases} z^{\delta} & ;\ \text{for}\ \ z \gg 1 \\ \text{const.} & ;\ \text{for}\ \ z \ll 1 \end{cases} . \tag{26}$$

The asymptotic form for $z \ll 1$ is due to the fact that the resonance function given by Eq. (9) does not depend on Ω if the time interval T is short because the sinc function in Eq. (9) has a broad peak for small T. The above asymptotic forms can be also confirmed by Eq. (9) and using the constant DOS near $\omega_{\rm F} = 0$. By fitting the calculated results of $\sigma(\omega, T)$ in Section 4 to the scaling function $G(z)$, one can estimate the exponent δ with high speed and accuracy.

Figure 2 shows the scaling function $G(z)$ defined in Eq. (25) for symplectic system. The most likely fit is determined by χ^2-statistic, and the confident intervals for fitting parameters were estimated from the Bootstrap procedure. The calculated results of the exponent is $\delta = 0.34 \pm 0.01$ for symplectic and orthogonal case, and $\delta = 0.34 \pm 0.02$ for unitary case, respectively. These values agree well with the prediction of the scaling theory for the ac conductivity $\sigma(\omega)$.[12)]

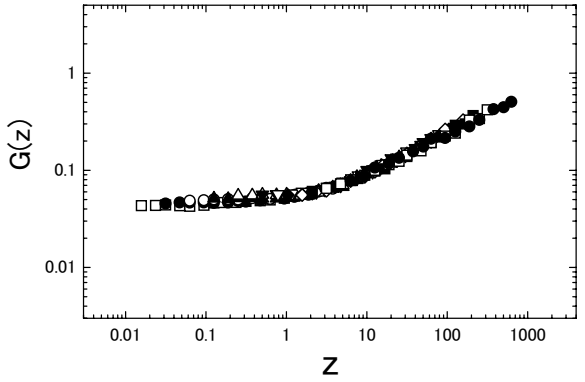

Fig. 2. The scaling function $G(z)$ for symplectic systems. The calculated results of the exponent is $\delta = 0.34 \pm 0.01$.

6. Summary

We have proposed a method for computing linear response functions for quantum systems described by large-scale Hamiltonian matrices. The method is based on solving the Schrödinger equation numerically in the presence of a generalized external force. We have furthermore presented the finite-time scaling method for computing the exponent of the frequency dependence $\sigma(\omega) \propto \omega^{\delta}$ near the Anderson transition. This method is especially powerful for evaluating the precise value of δ with high speed and accuracy. Although we have examined only conductivity problems, the present method is rather general, so it should be applicable for calculating various types of linear response functions. This issue is especially relevant in quantum systems in a variety of physical contexts.

We would like to thank Kousuke Yakubo for fruitful discussion. One of the authors (H.S) was supported in part by Research Fellowships of the Japan Society for the Promotion of Science for Young Scientists. This work was supported in part by a Grant-in-Aid for Scientific Research from the Japan Ministry of Education, Science and Culture. Numerical calculations were performed on the FACOM VPP 500 of the Supercomputer Center, Institute of Solid State Physics, University of Tokyo.

References

1) M. L. Williams and H. J. Maris: Phys. Rev. B **31**, 4508 (1985).
2) K. Yakubo, T. Nakayama, and H. J. Maris: J. Phys. Soc. Jpn. **60**, 3249 (1991).
3) T. Terao, K. Yakubo, and T. Nakayama: Phys. Rev. E **50**, 566 (1994).
4) T. Nakayama: in *Computational Physics as a New Frontier in Condensed Matter Research*, edited by H. Takayama et al. (The Physical Society of Japan, Tokyo, 1995), p. 21.
5) T. Nakayama and H. Shima: Phys. Rev. E **58**, 3984 (1998).
6) H. Shima and T. Nakayama: J. Phys. Soc. Jpn. **67**, 2189 (1998).
7) H. Shima and T. Nakayama: Phys. Rev. B **60**, 14066 (1999).
8) A. D. Greenwood: Proc. Phys. Soc. London **71**, 585 (1958).
9) R. Kubo: J. Phys. Soc. Jpn. **12**, 570 (1957).
10) P. W. Anderson: Phys. Rev. **109**, 1492 (1958); E. Abrahams et al.: Phys. Rev. Lett. **42**, 673 (1979).
11) F. J. Dyson: J. Math. Phys. **3**, 140 (1962); J. Math. Phys. **3**, 157 (1962); J. Math. Phys. **3**, 166 (1962).
12) F. J. Wegner: Z. Phys. B **25**, 327 (1976).
13) P. Lambrianides and H. B. Shore: Phys. Rev. B **50**, 7268 (1994).
14) K. Slevin, J. -L. Pichard, and P. A. Mello: J. Phys. (France) I **6**, 529 (1996).
15) A. MacKinnon and B. Kramer: Phys. Rev. Lett. **47**, 1546 (1981).
16) M. Henneke, B. Kramer, and T. Ohtsuki: Europhys. Lett. **27**, 389 (1994).
17) T. Kawarabayashi et al.: Phys. Rev. Lett. **77**, 3593 (1996).